GKSS

Testing a statistical method of global mean palotemperature estimations in a long climate simulation

Authors:

E. Zorita

F. Gonzalez-Rouco

GKSS 2001/25

DISCLAIMER

Portions of this document may be illegible in electronic image products. Images are produced from the best available original document.

GKSS 2001/25

Testing a statistical method of global mean palotemperature estimations in a long climate simulation

Authors:
E. Zorita
F. Gonzalez-Rouco
(Institute of Hydrophysics)

GKSS-Forschungszentrum Geesthacht GmbH • Geesthacht • 2001

Die Berichte der GKSS werden kostenlos abgegeben.
The delivery of the GKSS reports is free of charge.

Anforderungen/Requests:

GKSS-Forschungszentrum Geesthacht GmbH
Bibliothek/Library
Postfach 11 60
D-21494 Geesthacht
Germany
Fax.: (49) 04152/871717

ISSN 0344-9629

GKSS-Forschungszentrum Geesthacht GmbH · Telefon (04152)87-0
Max-Planck-Straße · D-21502 Geesthacht/Postfach 11 60 · D-21494 Geesthacht

GKSS 2001/25

Testing a statistical method of global mean palotemperature estimations in a long climate simulation

Eduardo Zorita, Fidel Gonzalez-Rouco

24 pages with 6 figures

Abstract

Current statistical methods of reconstructing the climate of the last centuries are based on statistical models linking climate observations (temperature, sea-level-pressure) and proxy-climate data (tree-ring chronologies, ice-cores isotope concentrations, varved sediments, etc.). These models are calibrated in the instrumental period, and the longer time series of proxy data are then used to estimate the past evolution of the climate variables. Using such methods the global mean temperature of the last 600 years has been recently estimated. In this work this method of reconstruction is tested using data from a very long simulation with a climate model. This testing allows to estimate the errors of the estimations as a function of the number of proxy data and the time scale at which the estimations are probably reliable.

Überprüfung einer statistischen Methode zur Abschätzung globaler Palaeotemperatur in einer langen Klimasimulation

Zusammenfassung

Die aktuellen statistischen Methoden zur Rekonstruktion des Klimas der letzen Jahrhunderte basieren auf stastistischen Modellen, die den Zusammenhang zwischen beobachteten Klimadaten (Temperatur, Luftdruck usw.) und stellvertretenden Klimadaten (u.a. Baumringdaten, Isotopenkonzentrationen in Eisbohrkernen, laminierten Sedimenten usw.) beschreiben. Diese Modelle werden im Beobachtungszeitraum kalibriert, und die längeren Zeitreihen der stellvertretenden Klimadaten werden dann dazu benutzt, die vergangene Entwicklung der Klimavariablen abzuschätzen. Mit einer dieser Methoden wurde jüngst die jährliche globale Temperatur der letzten 600 Jahren abgeschätzt. In dieser Arbeit wird diese Rekonstruktionsmethode mit Daten aus einer Simulation mit einem globalen Klimamodell getestet. Dabei wird der Schätzfehler als Funktion der Zahl der stellvertretenden Klimadaten und die minimale Zeitskala für eine zuverlässige Rekonstruktion untersucht.

Manuscript received / Manuskripteingang in TDB: 24. Juli 2001

Contents

1 Introduction

The observed increased of global mean air temperatures in the last 100 years has stimulated a great deal of efforts in the reconstruction of climate conditions in the past centuries, with the objective of putting the observed global warming into the perspective of the natural climate variability. These climate reconstructions may be based on simulations with climate models of different degrees of complexity (Cubash, 1997; Crowley, 2000) but also in the analysis of climate proxy data, such as tree-ring chronologies (Mann et al, 1998, Cook et al,1998), ice-core snow deposition rates (Appenzeller et al, 1998), or documentary evidence (Pfister et al, 1999).

Perhaps the most successful ones so far have been the estimation of past temperature (Mann et al., 1998) and sea-level-pressure (Luterbacher et al, 1999) evolutions by the use of statistical models linking a variety of climatic proxy data and the climatic variable of interest. These statistical models are set-up and validated in the instrumental period where both types of data sets overlap. The estimations of the evolution of the climate parameters are then performed by feeding these statistical models with the much longer time series of proxy data available. A good example of this strategy is the global annual temperature reconstructions of the last 600 years based essentially on a network of tree-ring chronologies, ice-cores in Greenland and other glaciers and very long instrumental time series by Mann et al. (1998). These authors employ a regression model that links the time series of the leading principal components of the global annual temperature field with the time series of the proxy data. The statistical model is validated using independent data from the instrumental period reserved for this purpose.

Although the methodology for this reconstructions is probably the best strategy that can be used in view of the data set available, several uncertainties may remain that are not easily resolved with the sole use of observational or proxy data sets, and that may require the analysis of long simulations of with coupled climate models. One of these uncertainties is related to the mismatch between the time scales of the model set-up and the time scale of the reconstructions. The statistical regression model can only be fitted and validated by necessity in the instrumental period, which optimistically can be considered as spanning about the last 150 years. However, other climate process operating on longer time scales may become more important for temperature variations than the short-term variations that exert most influence

in the values of the model parameters. The question then arises if the regression equations are still valid at these longer time scales. A second uncertainty comprises the number of climate proxy-data available. In most of the reconstructions based in statistical methods the number of proxy-data available decreases backwards in time. For instance in the study by Mann et al (1998), the number of proxy records available for the temperature reconstruction decreases from 112 in the period 1820 AD onwards, down to 22 in the period 1400-1450 AD. In the North Atlantic sea-level-pressure reconstruction by Luterbacher et al (1999), the number of proxies delivering informations from 1650 AD is 20% of the number of proxies available for 1900 AD..

Two questions can be posed in this context. One involves the minimum number of climate proxy records required for a meaningful reconstruction of the global temperature field. The second question concerns how the temperature reconstruction depend on the subset of proxy-indicators that is still available for the longest reconstructions. This subset is more a less a random group of the original set of proxies available and it could be reasonably argued that when the size of this subset decreases substantially the reconstructed temperature may be also depend on the (random) composition of this proxy subset.

In this paper we try to give an estimation of the uncertainties associated to these questions. Our objective is not to test the temperature reconstructions with a simulation with a global climate model driven by the estimated past variations of external forcing, such as solar variability, volcanic aerosols, etc. Our aims are rather to test if the statistical methodology remains valid for the estimation of global annual temperature at long-time scales in a complicated system, such as a coupled global climate model; to reach an estimation of the number of proxies required for a reasonable temperature reconstruction; and finally to investigate if the errors in the temperature reconstruction are equally distributed over the globe or if there exist regions where the temperature variations cannot be captured by the network of proxy data.

For our purposes a 1000 year long global climate simulation with a state of the art climate model will be analysed. The output of this simulation will play the role of pseudo climate, the temperature of which will reconstructed by a statistical regression model and a set of pseudo proxy data. Contrary to the real world, in a climate simulation no proxy data exist and, therefore, in this study the simulated temperature at selected grid-points will play the role of pseudo climate indicators. Our statistical model will therefore be set up between the simulated

global temperature field and those pseudo- indicators. In these approach several factors will contribute to a higher skill of the statistical climate model in the pseudo world of the climate model compared to the statistical model of the real climate. One factor is the relationship between the climate proxy data (e.g. tree-ring chronologies) and the local temperature at the position of the proxy time series. These relationships is known as the *transfer functions*, which in most cases are derived empirically and are therefore approximate and describe only part of the temperature variability. Our approach neglects completely this source of uncertainty. A second difference to the real world is the non-existence of external sources of climate variability, such as changes in solar output, that may be potentially affect the validity of the statistical model at long time scales. This aspect will be taken into account in a twin climate simulation with external forcing currently under way. A third question is the number of physical degrees of freedom present in a climate model. Because of the known limitation of computing power this number is clearly just a small fraction of the number of degrees of freedom of the real climate and, therefore, a statistical model linking climate variables within the climate simulation will probably tend to perform much better that its counterpart in the real world.

For these reasons the present study can be viewed as a test for the methodology of statistical climate reconstruction in clearly favorable conditions. The obvious advantage of analyzing a climate simulation with this purpose is that the state of the climate is completely known at all stages and the errors in the temperature reconstructed by the statistical model can be easily compared with the *true* (model simulated) temperature and the source of errors can be much more easily investigated.

The paper is structured as follows: a short description of the model and the climate simulation is given first. In section 3 a brief description of the statistical regression model and the data used to set up the model is included. The section 4 focuses on performance of the model as the number of proxy indicators is varied and the spatial differences in the temperature reconstructions. The paper is closed by the conclusions and suggestions for further work along these lines.

2 Model simulation

The global climate model consists of the spectral atmospheric model ECHAM4 developed at the German Climate Computing Centre (DKRZ). It has a horizontal resolution of T30 (aprox. 3.75°x 3.75°and 19 vertical levels. The atmospheric model is coupled to the ocean model HOPE-G also developed at the DKRZ (Legutke and Voss, 1999). The horizontal resolution of the ocean model is about 2.8°x 2.8 °with a grid refinement in the tropical regions, where the merdidional grid-point separation decreases progresively to the equator, reaching a value of 0.5°. This increased resolution allows for instance for a more realistic representation of ENSO events. The ocean model has 20 vertical levels. To avoid climate drift in such a long simulation the fluxes between both models are adjusted trough flux correction. The coupled model is driven by constant external forcing (solar constant and atmospheric concentrations of anthropogenic greenhouse gases), so that the variability is only due to the model internal dynamics. From this integration only the 2-m temperature field has been used in this study. The globally averaged annual temperature shows a stable behaviour with a range of variability of about 0.15 K . Regionally, the temperature variability can be larger and for instance in the European region, there exists periods several decades long, where winter temperature deviations reach 0.5 K, comparable to the ones observed in the Little Ice Age (Pfister ate al., 1999).

3 Statistical method for temperature reconstruction

The statistical method for the temperature reconstruction used by Mann el at (1998) is based on the calibration of regression equations between climate proxy time series, mainly dendrochronological data, and the principal components (PCs) of the annual temperature field over the globe. Once the statistical regression model has been calibrated using data from the instrumental period, it can be used to derive estimations of the amplitudes of the temperature PCs along the period with proxy data available. These amplitudes can be then used to reconstruct the global temperature field.

Since the number of locations where proxy data are available is limited, one can only expect to reconstruct the large-scale structures of temperature variability. In the most remote periods in the past, when only a few proxy data can be used only the leading PC is expected to be

reasonably well estimated. In this study we have used the same method as in Mann et al (1998).

Since the climate model obviously does not simulate climate proxy records, the air-temperatures simulated at the grid points most closely situated to the locations of the proxy records are taken as the "simulated proxies". This approach neglects all the sources of errors inherent to the statistical transfer functions between the proxy record and the local climate conditions. These source of errors can be quite large and strongly dependent of the location and the nature of the proxy. The focus of this study lies, however, in testing if a reasonable number of proxy records is in principle sufficient for realistic reconstructions of a global temperature field.

The model is calibrated in the reference period between the simulated years 800 and 1000. First, an Empirical Orthogonal Function Analysis of the standardized temperature anomalies is carried out:

$$T(x_i,t) = \sum_{j=1}^{N} f_j(x_i)\alpha_j(t) \tag{1}$$

where $T(x_i,t)$ is the standardized temperature anomaly at grid point x_i in the model years 800 - 1000, N is the number of grid points, f_j is the j^{th}Empirical Orthogonal Function and α_j is the corresponding principal component. The spatial patterns f_j are the eigenvectors of the weighted correlation matrix of the temperature field, where the weights represent the latitudinally varying surface of each grid box. Since the patterns f_j are eigenvectors, their normalization is arbitrary. Here, the normalization is chosen so that the standard deviation of the principal components α_j in the calibration period is unity.

In a second step a multiple linear regression equation linking the leading principal components (as predictor) and the standardize anomalies of local "proxy" data (as predictand) is set up:

$$p_k(t) = \sum_{j=1}^{n} a_k^j \alpha_k(t) + \epsilon_k(t) \tag{2}$$

where $p_k(t)$ is the standarized anomaly of the k^{th}proxy, a_k^j are the regression coefficients and ϵ are the residuals. Since the time mean of the proxies and of the pcs in the calibration period is zero, no independent term is needed in the regression model. The number of proxies ranges in this study between 84 and 15, whereas the number of considered leading EOFs is of

the order of 10 or less, so that the regression model defined in equation 2 is always well posed. The value of the coefficients a_k^j can be estimated by minimizing the total variance of ϵ_k .

Once the coefficients a_k^j have been estimated in the calibration period the model can be reversed to estimate temperature deviations when the value of the proxy data (in our case the temperature at the proxy grid-points) is known. First, equation 2 can be solved for each year setting the value of the residuals to zero, yielding an estimation of the amplitude of the principal components $\alpha(t)$ at year t that best replicate the value of the proxy records. In a second step the standarized temperature field can be reconstructed by setting in the estimated values of $\alpha(t)$ in equation 1. Finally, the physical temperature field is obtained by multiplying at each grid-point the reconstructed standarized field by the grid-point standard deviation estimated in the period of calibration. It should be noted that this reconstruction method yields an estimation of the value of the temperature principal components that is optimal for the set of climate indicators as a whole, and that the estimations of individual principal components cannot be traced back to a particular subset of indicators or to an individual climate indicator. This fact has the advantage that possible errors in particular indicators are not critical, since the signal is extracted from all the indicators simultaneously.

Several measures can be used to asses the quality of the reconstructed temperature field. Measures that keep the spatial information can be the local time correlation between the simulated and reconstructed temperature or the Brier skill score, also known as percentage of explained (or resolved) variance, defined as:

$$\beta_i = 1 - \frac{\sum_t (T_{sim}(x_i,t) - T_{rec}(x_i,t))^2}{\sum_t T(x_i,t)^2} \tag{3}$$

where T_{sim} is the temperature deviations from the mean of the calibration period, T_{rec} is the reconstructed temperature deviations and i is the grid-point index.

The leading four Empirical Orthogonal Functions (EOFs) of the annual temperature field simulated by the ECHO-G model in this control integration in the period between the simulation years 800 and 1000 are shown in Figure 1. The leading EOF shows temperature anomalies of the same sign in North America, South America and Antarctica and temperature anomalies of opposite sign in Eurasia. The second EOF describes essentially strong temperature anomalies along the Equatorial Pacific associated with an ENSO event, which underlines the ability

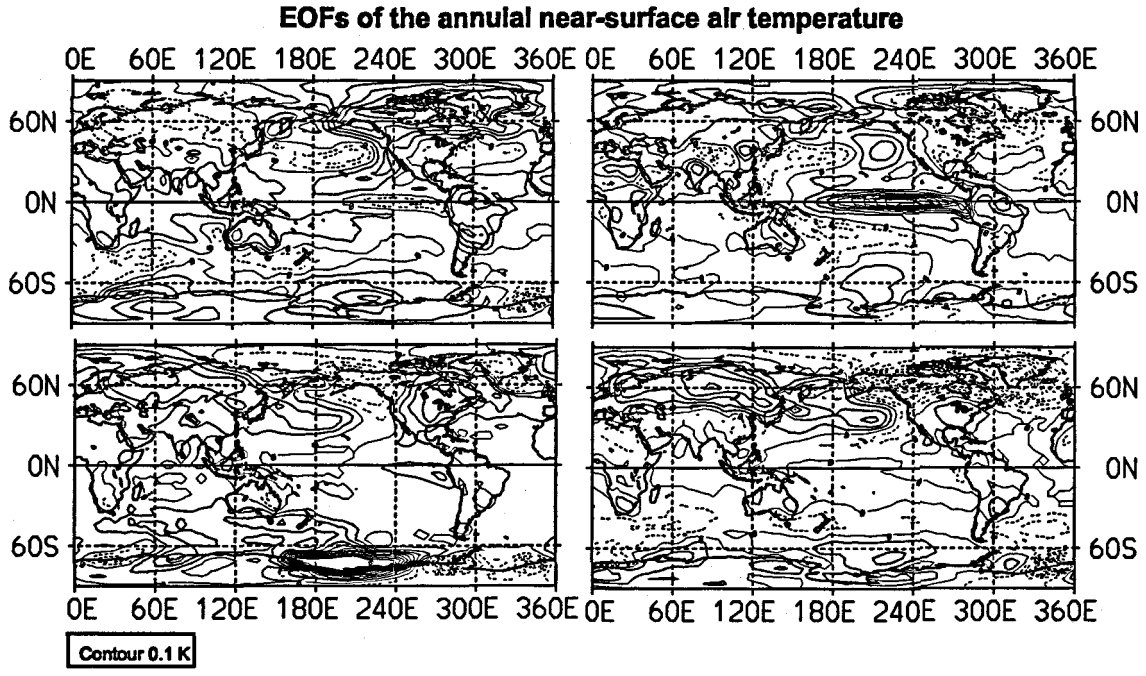

Figure 1: The four leading Empirical Orthogonal Function of the global mean annual temperature in the control simulation with ECHO-G. Dashed lines indicate negative values. Contour interval is 0.1 K.

of the ECHO global model in simulating the Tropical Pacific variability. The temperature anomalies associated with the third EOF show strong values in the Pacific Antarctic sector and slightly weaker anomalies in North America and Eurasia. The fourth EOF describes a temperature contrast between Eurasia on one side and Greenland and Northern North America on the other side. This principal component of this fourth EOF is strongly correlated (r=0.63) with the Arctic Oscillation index in the model simulation. In this case the Arctic Oscillation is defined as the leading EOF of the annual mean sea-level-pressure field in the Norther Hemisphere, and shows the well known centers of action with alternating signs in the North Atlantic at mid-latitudes, Greenland and the North Pacific. Only the principal components of the first and third EOF are strongly correlated with the global mean temperature (r=.53 and r=.64 respectively). Both together can therefore describe 70% of the variability of the global annual mean temperature.

However, a clear difference with the temperature EOFs derived from observations (Mann

et al, 1998) is that no spatial pattern shows essentially the same sign over the whole globe. This fact can be due to the lack of external forcing in this simulation. In the real world at least two factors, greenhouse gas atmospheric concentrations and solar variability, contribute to a global in-phase variations of temperature. However, other control simulations performed with other models (Stouffer et al, 2000) do show a leading air temperature EOF with a almost uniform sign over the globe.

4 Dependence of the temperature reconstructions on the number of proxies used

As stated before, the role of climate proxy data will be played by the simulated air-temperature at the grid points most closely situated to the locations of the proxies used in Mann et al (1998). The number proxies used by these authors depends on the period where the reconstruction is attempted, since not all proxy data are available throughout the whole period back to 1400 AD. In the most recent period a number of 112 indicators was used. Since the horizontal resolution of the ECHAM model in this simulation is rather coarse (about 3.75 °) some of the locations of these indicators have to be associated to the same grid point in the model. Therefore, in this study the maximum number of pseudo-indicators is limited to 84. The position of the grid-points playing the role of climate indicators is shown in figure 2. The pseudo-indicators are therefore the annual near-surface air temperature in these 84 grid points. It can be seen that most of the pseudo-indicators are situated in the Northern Hemisphere over land. Those originally located on islands now correspond to ocean-grid points, but this difference should not be critical, since the relationships of the local to the large-scale temperature fields would be probably very similar to the case that small islands were resolve in the climate model. No pseudo indicator is located in Antarctica.

The calibration period was chosen to be the last 200 years of the climate simulation. This choice should be arbitrary as far as it is far enough from the spin-up phase of both components of the climate model. The choice was somehow dictated by the relatively sharp increase of global mean temperature seen in the last decades of the simulation, which in some sense could play the role of the global warming observed in the real world in the last 100 hundred years,

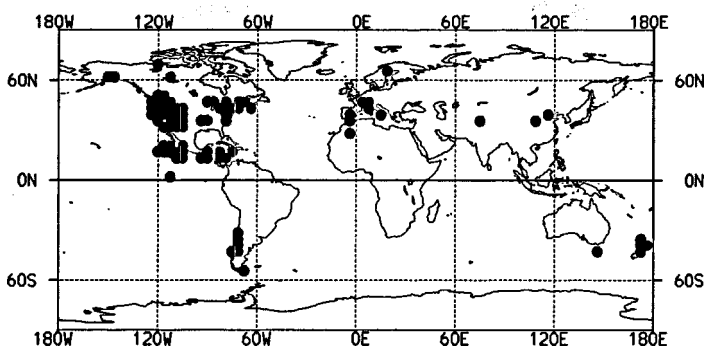

Figure 2: Position of the grid-points in the climate model ECHO at a resolution T30 most closely located to the proxy indicators in Mann et al. (1998).

although of a smaller magnitude. The calibration period in Mann et al (1998) obviously lies within the observed global warming phase.

The simulated annual temperature field throughout the whole simulation can be reconstructed once a set of pseudo-indicators has been chosen. To estimate the influence of the number of pseudo-proxies used in the reconstruction, the reconstruction method was applied using a decreasing number of pseudo- indicators n_{pi}, ranging from the original number $n_{pi} = 84$ down to $n_{pi} = 15$. In the real reconstruction by Mann et al. (1998) the set of proxy data remaining backwards in time is given by extarnal and independet factors, such as archeological investigations on favorable tree-ring sites, and therrefore this set is presumably a random selection of the original proxy data set. To mimic this situation, for each value of n_{pi}, ensemble reconstructions of 50 members each were carried out, where n_{pi} pseudo-indicators were chosen at random from the original set of 84. For each member of the ensemble, the reconstructed temperature was globally averaged and compared directly with the simulated global annual temperature.

Figure 3 shows the ensemble mean explain variance as a function of the number of pseudo-indicators. It can be seen that the mean explained variance drops, as expected, with decreasing number of pseudo- indicators. The explained variance attains values greater than one (i.e. the mean squared error is less that the temperature variance) for $n_{pi} > 50$. For values of n_{pi} of the order of 20 the mean squared error of the reconstruction is about a factor 1.2 larger than the simulated temperature variance.

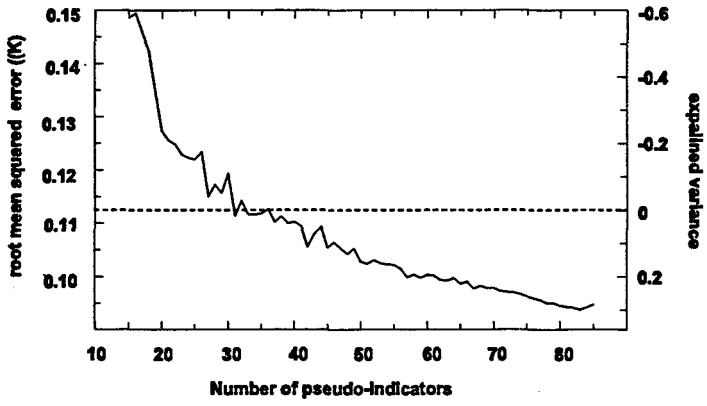

Figure 3: Mean squared error of the reconstructed annual global temperature as a function of the number of pseudo-indicators.The Breir skill score (percentage of explained variance) is also indicated

Also interesting is the question if the errors of the temperature reconstruction are distributed uniformly over time or if there are some periods where the errors tend to be larger than in other periods, regardless of the number of pseudo-indicators. This would indicate a systematic deficiency of the method in capturing certain climatic configurations better than others. Figure 4 shows the ensemble mean of the mean square error of the temperature reconstruction as a function of simulated time for $n_{pi} = 50$ and $n_{pi} = 15$ filtered by a 20-year-running mean. The mean errors are, as expected, larger when only 15 pseudo-indicators are used, but it can be seen that there are common periods where the errors tend to be larger for both sizes of pseudo-indicator predictor set. Figure 4 also shows as illustration a filtered version (20-year running mean) of one member of each ensemble of reconstructions. It seems clear that the reconstruction error evolve in parallel for $n_{pi} = 50$ and $n_{pi} = 15$ and that in the periods when the errors tend to be larger, the simulated global mean temperature tends to be cooler than the reconstructed global temperature. These periods are the first 100 years of the climate simulation and the periods 380-410 and 580-600, also marked in figure 4.

The reasons why the periods of larger reconstructions errors occur when the simulated temperature is overestimated can be investigated by estimating the spatial anomaly fields of key variables that are associated with the reconstruction errors. A possible way is to construct the regression map of several climate variables taking the time series of ensemble mean squared

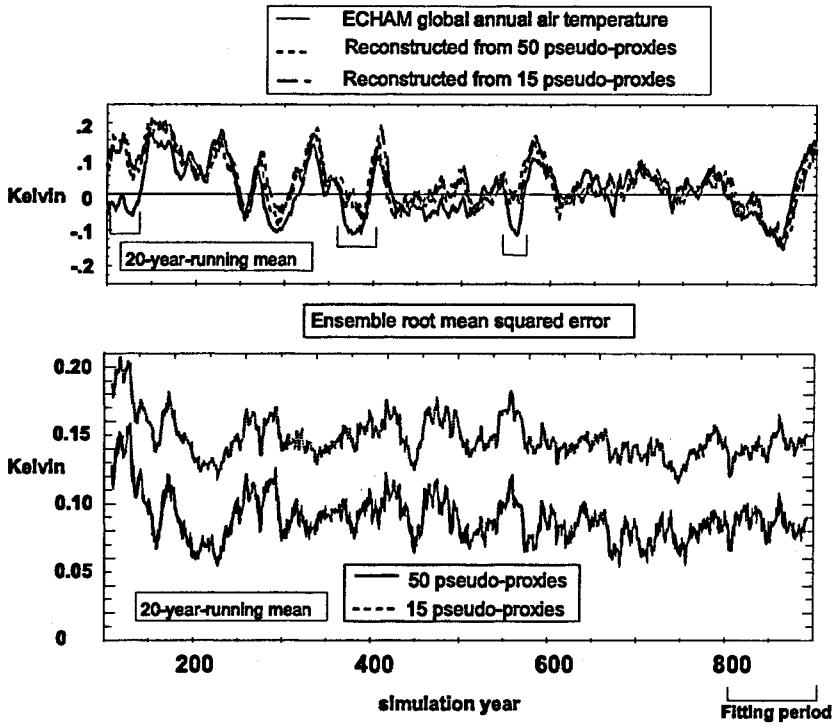

Figure 4: Upper panel: Simulated global mean annual temperature and one statistical temperature reconstruction with 50 and 15 pseudo-indicators. Lower pannel: Ensemble mean squared error of the annual global mean temperature reconstructions along the simulation when using 50 and 15 pseudo-indicators. The fitting period is also indicated.

error (Fig.4a) as the basis time series, as indicated in the following equation:

$$r_f(x_i) = \frac{1}{N}\sum_t f(x_i,t)\gamma_{rms}(t) \tag{4}$$

where r_f is the regression map for variable f and γ is the standarized time series of the ensemble mean squared error (Figure 4a).

These regression maps for near-surface air temperature, geopotential height at 500 mb and fractional sea-ice cover are shown in figure 5.

These maps indicate the typical anomalies of these fields when the time series of explained variance deviates one standard deviation from its mean value. This figure is based on a reconstruction with 50 pseudo-indicators, but it can be considered representative over a very broad range of $n_{pi} = 15$. The regression pattern obtained for air temperature is very similar

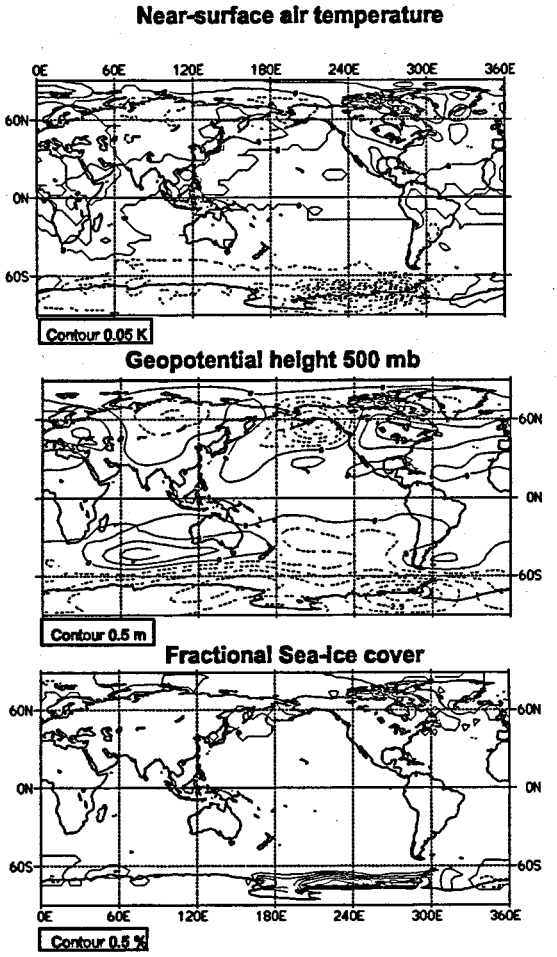

Figure 5: Maps of the simulated annual temperature (K, contour 0.05 K), mean annual geopotential height at 500 mb (m, contour 0.5 m) and fractional sea ice-cover (percent, contour 0.5%) regressed onto the time series of ensemble mean error of reconstructed temperature with 50 pseudo-indicators. (Fig. 4). Dashed isolines indicate negative values

to the spatial pattern of local mean squared difference between simulated and reconstructed temperature averaged along the whole simulation (not shown):

$$rms_T(x_i) = \frac{1}{N}\sqrt{\sum_t (T_{sim}(x_i,t) - T_{rec}(x_i,t))^2} \tag{5}$$

The temperature regression map attains its highest values in the Southern Hemisphere along the Antarctic coast, which, in view of the lack of pseudo- indicators in this part of the world, seems a reasonable result. In the periods where the errors are large the temperatures

in these regions tend to be colder that the time average. Actually, these colder temperatures are also reflected in the global annual mean (Fig. 4). The reconstructions fail to capture these temperature drops and overestimate the global mean temperature.

Figure 5 also show the regression maps of the annual mean geopotential height and sea-ice cover regressed onto the ensemble mean squared error of the temperature reconstruction. The geopotential regression map shows lower geopotential heights over Antarctica, so that the meridional geopotential gradient is increased relative to the mean climate. According to the thermal wind equations, this increased gradient should be associated with stronger westerlies in the Southern Hemisphere. Simultaneously, also consistently with the lower air temperatures, sea-ice tends to cover a larger region in the Pacific sector of the Antarctic Ocean.

It seems therefore that there exist a temperature variability configuration in the ECHO model over the Antarctic continent that is also associated to consistent variations of the geoptential height (and accordingly, also to intensities of the westerlies in the Southern Oceans) and sea ice cover. This configuration is not properly grasped by the network of pseudo-proxies, mainly located in the Northern Hemisphere over land. It should not be forgotten that this variability mode could be just a feature of the ECHO model and not necessarily a variability mode of the real climate. A more throughout physical analysis of this variability mode is beyond the scope of this paper.

It could be argued that the inclusion of pseudo-proxies in Antarctica could improve this deficiency. A reasonable number of pseudo-proxies that could be included would be, however, limited to just a few, in view of the locations were ice-cores have been drilled so far. This small number would be outweighted by the remaining 50 (or in the whole set of 84) pseudo-indicators. Since the statistiscal model is design to find the best estimated temperature that would be optimally consistent with all pseuo-indicators at the same time this estimation would be very little influenced by the inclusion of a few additional pseudo-indicators in Antarctica. In fact, this is the case (not shown) when 3 pseudo indicators located in Antarctica are included in the pseudo-indicator set after the Montercarlo resampling (i.e. they are always present in the regression model). For these Antarctic pseudo-indicators to have a real influence on the estimations, the regression model would have to be modified to artificially weight each pseudo-indicator by the area that it presumably represents, so that three Anctarctic pseudo-indicators

have the same weigth in the estimation process as, say , all European pseudo-indivators. . In many cases the area corresponding to each pseudo-indicators would have to be estimated somewhat subjectively.

5 Spectral characteristics of the temperature reconstruction

The exercises shown so far in this paper aim at the reconstruction of the global mean temperature on an annual time scales, based on annual time series of pseudo-indicators. However, in many paleoclimatic studies the interest lies not in climate reconstructions at such short time scales, but on longer periods. Usually the time resolution of the reconstructions is dictated by the availability of adequate proxy data, but also the interest is naturally shifted to the decadal or centennial time scales. At these long time scales, the fraction of variance explained by the temperature reconstruction will tend to increase, since probably the lower frequency process responsible for temperature variations will tend to influence the whole globe simultaneously.

Figure 6 shows the coherence spectra between the reconstructed and simulated global annual temperature. It can be seen that the reconstructions with 50 pseudo-indicators the coherence remains more or less at a constant level (around 0.5, corresponding to an explained variance of 25%) from the interannual times scales up to about time scales of 5 years. For longer time scales the coherence increases up to the lowest resolved frequency. For these long time scales the coherence reaches about 0.8 (about 60% of explained variance). A similar behaviour is observed for the reconstruction with 15 pseudo-indicators, although the coherence is, as expected, always lower than for 50 pseudo-indicators. This result underlines the potential for the estimation of past natural global temperature variability with a relatively small numer of proxy indicators at time scales of decades, which is the relevant time scale for studies of detecion of climate change in the observational record.

These result may indicate that at decadal time scales the number of indicators required for a reasonable reconstruction of the global mean temperature can be much lower than at interannual time scales. the spectra shown in Figure 6 are the ensemble mean of all 50 Montecarlo reconstructions. Probably, if the location of the pseudo-indicators were to be chosen in a sensible way higher coherence may be achieved with the same number of pseudo-indicators.

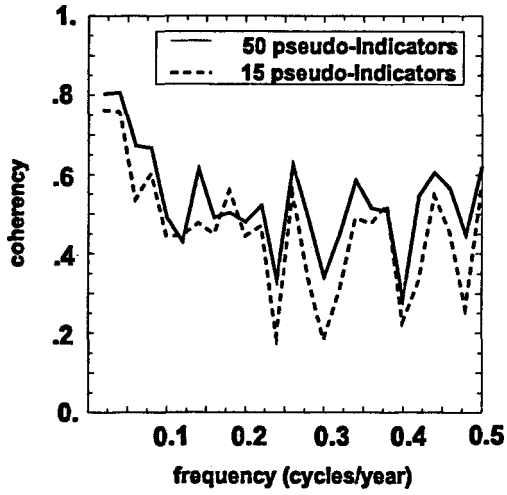

Figure 6: Coherence between the simulated and reconstructed (50 pseudo-indicators and 15 pseudo-indicators) annual global mean temperature.

However the choice of optimal pseudo-indicators is likely to be dependent on the system under study, in this case the ECHO model, and may not be directly transferable to the real climate.

6 Conclusions

The aim of empirical models linking local proxy indicators and large-scale climate indices, such as the annual global mean temperature, is to estimate past evolution of these large-scale indices. In this paper a reconstruction exercise has been performed with in the world simulated by a global climate model, where the role of the pseudo-indicators has been played by air temperature simulated at selected grid points.

There are at least two sources of uncertainty in the real climate reconstructions: one is given by the empirical transfer function between the real proxy indicators and the real local climatic conditions; the second has its origin in the statistical reconstruction model itself. In our exercise only the last source of uncertainty can be quantified; in the real world the reconstructions errors are likely to be higher.

In the climate simulated by the ECHO model without external forcing the global annual mean temperature can be reasonably reconstructed with about 50 pseudo-proxy indicators

placed in the locations of a reasonable network of real proxy-indicators. Although the empirical model has been fitted with annual data, the lower-frequency variations of the global mean temperature are reproduced in a validation period.

Some deficiencies related to the irregular distributions of pseudo-indicators remain. The highest deviations between model-simulated and reconstructed temperature are related to the inability of the empirical model in describing temperature variations over Antarctica. In those case the reconstructed temperature is always an overestimation of the simulated temperature. These periods of lower than normal temperatures over Antarctica are associated with increased sea-ice cover in the Pacific sector of the Southern Oceans and stronger westerlies at mid-latitudes in the Southern Hemisphere. Since this particular statistical model is designed to optimally use the information contained in all pseudo-indicators *simultaneously*, the inclusion of more pseudo-proxies located in or near Antarctica cannot improve the situation, since the weight of the (reasonably) few Antarctica pseudo-indicators would be low in a set of, say, 50 pseudo-indicators.

The skill of the statistical model increases at longer time scales. The coherence of the simulated and reconstructed global annual temperature attains values around 0.8 at time scales of 10 years even when only 15 pseudo-indicators are used. This fact suggest that if the interest lies in climate reconstructions at decadal time scales, perhaps a useful strategy is to identify real proxy indicators that are tightly connected to the local climate conditions, rather than to expand a network of proxy indicators, individually more loosely connected to their respective local climate.

References

Appenzeller C, Stocker TF, Anklin M, 1998: North Atlantic oscillation dynamics recorded in Greenland ice cores. Science **282**, 446-449

Cook ER, D'Arrigo RD, Briffa KR, 1998 A reconstruction of the North Atlantic Oscillation using tree-ring chronologies from North America and Europe. Holocene **8** 9-17.

Crowley. T.J., 2000: Causes of climate change over the last 1000 years. Science **289**, 270-277.

Cubasch U, Voss R, Hegerl GC, Waszkewitz J, Crowley TJ., 1997: Simulation of the influence of solar radiation variations on the global climate with an ocean-atmosphere general circulation model.Climate Dynamics **13**, 757-767.

Cubasch U, Voss R., 2000: The influence of total solar irradiance on climate Space Science Reviews , 94 (1-2): 185-198.

Jones PD, Briffa KR, Barnett TP, Tett SFB, 1998: High-resolution palaeoclimatic records for the last millennium: interpretation, integration and comparison with General Circulation Model control-run temperatures. Holocene **8** 455-471

Jones PD, Briffa KR, Barnett TP, Tett SFB, 1998: High-resolution palaeoclimatic records for the last millennium: interpretation, integration and comparison with General Circulation Model control-run temperatures. Holocene **8**, 455-471 (1998).

Jones, P.D., T.J. Osborn, T.J., and K.R. Briffa, 2001: The evolution of climate over the last millenium. Science **292** 662-667.

Legutke S, and R. Voss, 1999: ECHO-G, The Hamburg Atmosphere-Ocean Coupled Circulation Model. Deutsches KLimarechenzentrum Report No. 18. Available from Deutsches Klimarechenzentrum. Bundesstrasse 55 D-20146 Hamburg, or http://www.dkrz.de/forschung/reports.html.

Luterbacher J, Schmutz C, Gyalistras D, Xoplaki E, Wanner H, 1999: Reconstruction of monthly NAO and EU indices back to AD 1675. Geophys. Res. Letters **26** 2745-2748.

Mann ME, Bradley RS, Hughes MK, 1998: Global-scale temperature patterns and climate forcing over the past six centuries. Nature **392**, 779-787.

Pfister C, Brazdil R, Glaser R, Barriendos M, Camuffo D, Deutsch M, Dobrovolny P, Enzi S, Guidoboni E, Kotyza O, Militzer S, Racz L, Rodrigo FS, 1999: Documentary evidence on climate in sixteenth-century Europe. Climatic Change **43** 55-110.

Stouffer RJ, Hegerl G, Tett S, 2000: A comparison of surface air temperature variability in three 1000-yr coupled ocean-atmosphere model integrations. J. of Climate **13**, 513-537.

Thompson DWJ, Wallace JM, 1998 The Arctic Oscillation signature in the wintertime geopotential height and temperature fields. Geophys. Res. Letters **25**, 1297-1300.